Title

MODELING MOTION SICKNESS USING A FOUR-WHEEL VEHICLE MODEL AUGMENTED WITH A PASSENGER MODEL

Journal

2021 International Conference on Bond Graph Modeling and Simulation, ICBGM 2021, 53(3)

ISSN

07359276

Authors

Kim, Eunil
Akbari, Ali
Margolis, Donald

Publication Date

2021-11-10

Peer reviewed

MODELING MOTION SICKNESS USING A FOUR-WHEEL VEHICLE MODEL AUGMENTED WITH A PASSENGER MODEL

Eunil Kim
Hyundai Center of Excellence, Hwaseong-si, Gyeonggi-do, 18280, South Korea,
eunilk@hyundai.com

Ali Akbari And Donald L. Margolis
University of California Davis, Davis, California, 95616, US, alakbari@ucdavis.edu,
dlmargolis@ucdavis.edu

ABSTRACT

Motion sickness is being highlighted as one of the most significant ride comfort issues for autonomous vehicles. Studies have attributed the feeling of motion sickness to the lateral motion of the vehicle. Additional studies have addressed that there is a meaningful correlation between the lateral motion of a passenger's head with their feeling of motion sickness. Using bond graphs, a model of a vehicle with a sitting passenger on board is constructed which allows for computation of the vehicle's lateral and roll motion as well as the lateral and roll motion of the passenger's head. Furthermore, if the passenger's head motion is available, the Motion Sickness Incidence (MSI) can be calculated using available literature. The objective of this research is to estimate motion sickness from the head roll motion for future use in developing a suspension control that will mitigate motion sickness.

Keywords: motion sickness, ride comfort, vehicle dynamics, biomechanics, bond graph modeling

1 INTRODUCTION

As we are approaching the autonomous vehicle era, the issue of motion sickness is becoming more significant than ever. From the experience of daily life, we already know that passengers feel more motion sickness than drivers. It turns out that unpredictability can cause relatively severe motion sickness. When passing through a corner, drivers instinctively move their heads in the opposite direction of lateral acceleration since they can predict what will happen. However, this is harder for the passengers unless they maintain focus on the front. This makes a different severity of motion sickness between drivers and passengers (Wada et al. 2012). In an autonomous vehicle, all those who are on-board become passengers, not drivers. Therefore, motion sickness is amongst the most critical challenges which should be addressed in the future. There are many variables affecting motion sickness, including visual factors, olfactory factors, translational and rotational motion in each direction, and duration of the ride. Among these factors, this research focuses on figuring out the relationship between motion sickness and vehicle's lateral motion through simulation, such that a motion sickness index will be numerically given as a result. The SVC (Subjective Vertical Conflict) model (Wada et al. 2007; Wada and Kamiji 2015) is employed for the calculation of MSI (Motion sickness Incidence, %) from the passenger's head motion. If we know the lateral acceleration and roll rate of the passenger's head, we can then get an MSI as an objective result from the SVC model. The concept for modeling

ICBGM'2021 Nov 8-10, 2021- San Diego, California USA - ©2021 Society for Modeling & Simulation International (SCS)

motion sickness is summarized in Fig. 1. In this paper, an integrated model is presented which

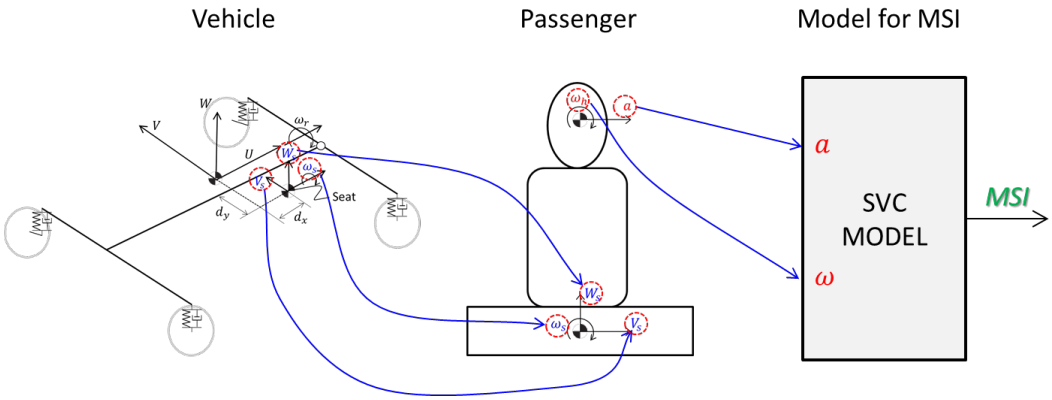

Figure 1: The concept for modeling motion sickness

combines a four-corner vehicle model augmented with an on-board passenger model using Bond graphs. Thereafter, simulation results will be verified against experimental results.

2 BOND GRAPH MODELING

2.1 Four-wheel vehicle model

A Four-Wheel vehicle model with four body degrees-of-freedom and a constant cruising velocity was used in this paper. All parameters for this vehicle model reflects a mid-sized sedan. Since only lateral motion is of interest, the model has no pitch motion, and the Dugoff Tire Model (Dugoff et al. 1970) is used to estimate tire forces in the nonlinear region. The Schematic of the vehicle model is shown in Fig. 2. To construct the model's bond graph, these kinematic equations are derived below:

For the Front:

$$\mathrm{U_{rf}} = U + \frac{w}{2}\cdot\omega_y\,,\quad V_{rf} = V + a\omega_y + \left(h_{cg} - h_{rc}\right)\cdot\omega_r \qquad \text{eq. (1,2)}$$

$$\mathrm{U_{lf}} = U - \frac{w}{2}\cdot\omega_y\,,\quad V_{lf} = V + a\omega_y + \left(h_{cg} - h_{rc}\right)\cdot\omega_r \qquad \text{eq. (3,4)}$$

$$\mathrm{W_{rf}} = W - \frac{w}{2}\cdot\omega_r,\quad \alpha_{rf} = \delta - \frac{V_{rf}}{U_{rf}} \qquad \text{eq. (5,6)}$$

$$\mathrm{W_{lf}} = W + \frac{w}{2}\cdot\omega_r,\quad \alpha_{lf} = \delta - \frac{V_{lf}}{U_{lf}} \qquad \text{eq. (7,8)}$$

For the Rear:

$$\mathrm{U_{rr}} = U + \frac{w}{2}\cdot\omega_y\,,\quad V_{rr} = V - b\omega_y + \left(h_{cg} - h_{rc}\right)\cdot\omega_r \qquad \text{eq. (9,10)}$$

$$\mathrm{U_{lr}} = U - \frac{w}{2}\cdot\omega_y\,,\quad V_{lr} = V - b\omega_y + \left(h_{cg} - h_{rc}\right)\cdot\omega_r \qquad \text{eq. (11,12)}$$

$$\mathrm{W_{rr}} = W - \frac{w}{2}\cdot\omega_r,\quad \alpha_{rr} = -\frac{V_{rr}}{U_{rr}} \qquad \text{eq. (13,14)}$$

$$\mathrm{W_{lr}} = W + \frac{w}{2}\cdot\omega_r,\quad \alpha_{lr} = -\frac{V_{lr}}{U_{lr}} \qquad \text{eq. (15,16)}$$

Where rf, lf, rr, lr subscripts denote right front, left front, right rear, and left rear corners, respectively. Also, U, V, W, ωy, ωr indicate the vehicle's longitudinal, lateral, heave, yaw (angular), roll (angular) velocities, respectively. δ is the steering angle input and α indicates the side slip angle at each corner. Lengths a and b are the front and rear axle's distance from the vehicle's center of gravity, w is the half-track length, hcg and hrc indicate the heights of the vehicle's center of gravity and roll center, respectively. The bond graphs for the front and rear are shown in Fig. 3 and Fig. 4. Given that the cruising speed is considered to be constant and no pitch motion is considered for the vehicle, the equations of motion for the main vehicle body would be derived as follows:

$$\dot{\mathrm{p}}_{\mathrm{yaw}} = J_y\dot{\omega}_y = \Sigma M_y \qquad eq.\,(17)$$

$$\dot{\mathrm{p}}_{\mathrm{roll}} = J_r\dot{\omega}_r = \Sigma M_r \qquad eq.\,(18)$$

$$\dot{\mathrm{p}}_{\mathrm{lat}} = m_T\dot{V} = \Sigma F_{lat} - \omega_y\cdot m_T\cdot U + \omega_r\cdot m_s\cdot W \qquad eq.\,(19)$$

$$\dot{\mathrm{p}}_{\mathrm{heave}} = m_s\dot{W} = \Sigma F_{heave} - \omega_r\cdot m_T\cdot V \qquad eq.\,(20)$$

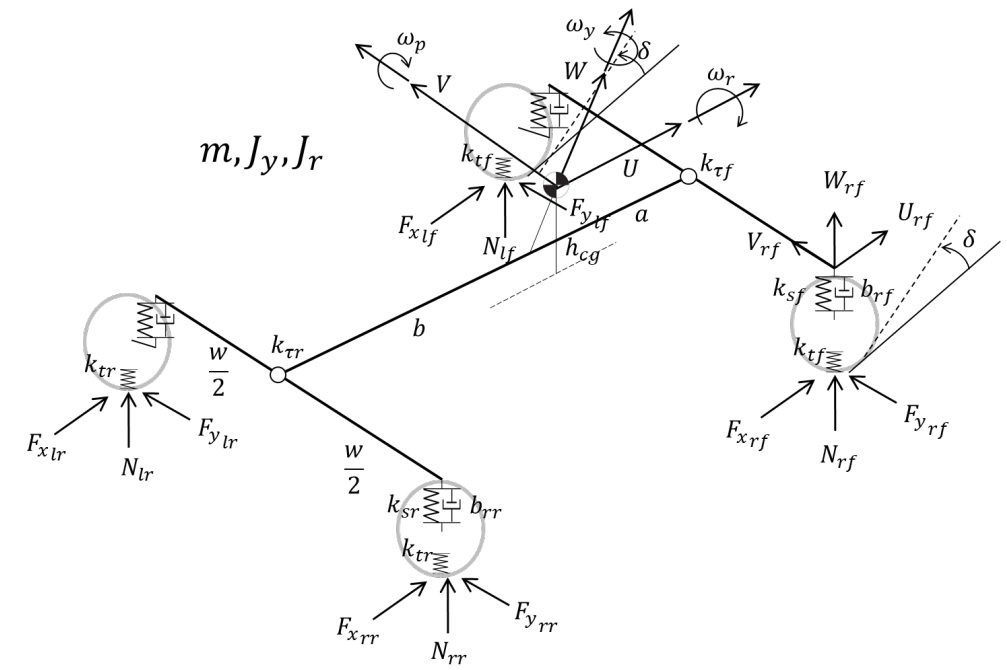

Figure 2: Schematic of the four-wheel vehicle model

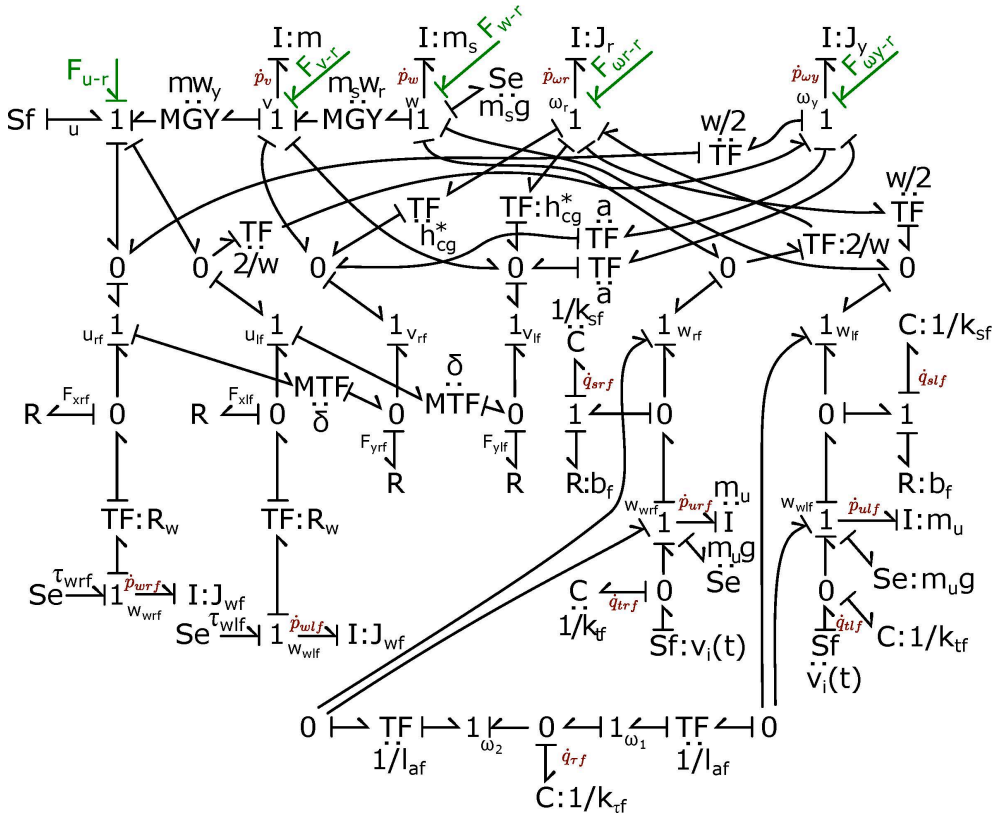

Figure 3: Bond graph of the front of the four-wheel vehicle model

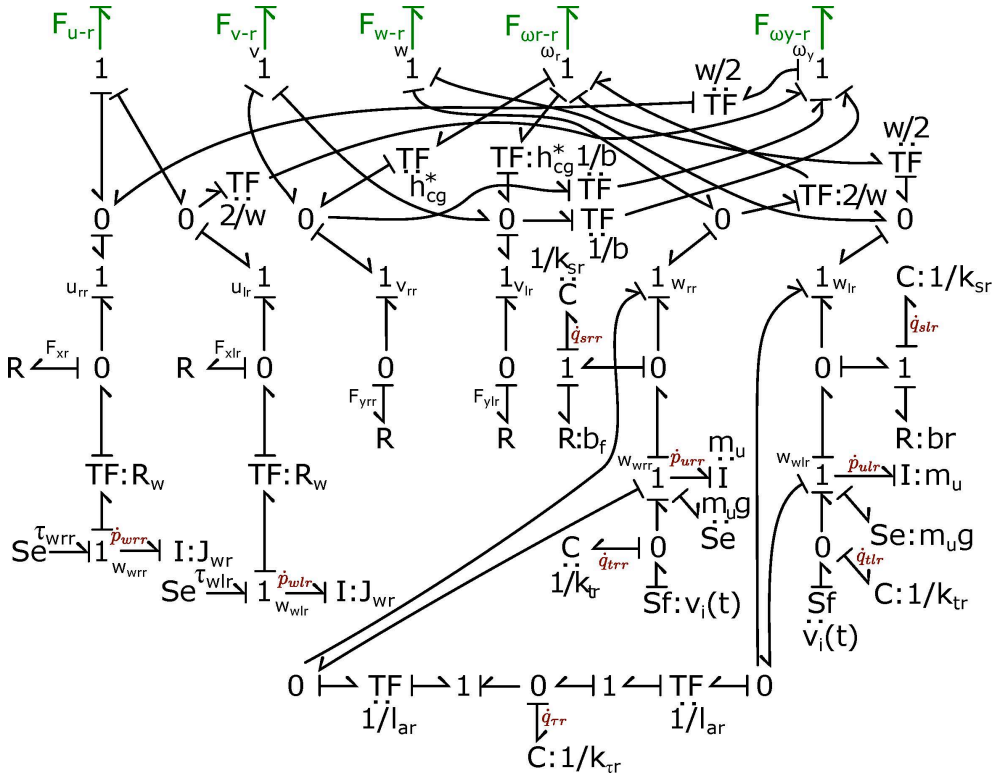

Figure 4: Bond graph of the rear of the four-wheel vehicle model

Where m_T, m_s, J_y, J_r indicate the vehicle's total mass, sprung mass, yaw moment of inertia, and oll moment of inertia, respectively $\Sigma M_y, \Sigma M_r, \Sigma F_{lat}, \Sigma F_{heave}$ denote moment sums and force sums in their respective directions and are found according to the bond graph.

Although the front and rear bond graphs for the vehicle model are presented separately, the two ond graphs are connected to one another. The green arrows and variables in said bond graphs indicate the front-rear connection.

2.2 **Passenger body model**

For calculating the MSI as the quantitative index of motion sickness, information on the passenger's head motion is required. Wu et al. (Wu, Jun, and Yi Qiu 2020) developed the concept for a 12 degrees-of-freedom passenger model, which assumes separate modules for the head, upper torso, lower torso, and buttocks. All modules have independent lateral, heave, and roll motions. Also lateral, vertical, and torsional compliance is considered between each two consecutive modules. A back seat is also modeled which provides compliance between the seat and the lower torso in lateral, vertical, and torsional directions. The velocities of the seat which serve as input to the passenger model come from the vehicle model,

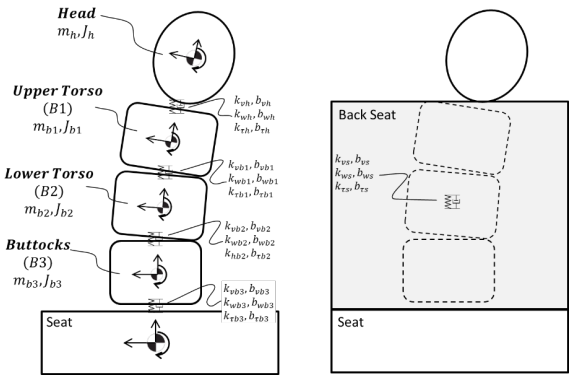

Figure 5: 12 degree-of-freedom passenger model

after accounting for the offset from the passenger's sitting location from the vehicle's center of gravity using velocity transfer. The output from the passenger model will be the passenger's head motion. The schematic for the passenger model is shown in Fig. 5.

To make the passenger model's bond graph, relative velocities across compliant elements are:

$$V_{rel,h} = (V_{B1} - \frac{h_{b1}}{2} \cdot \omega_{B1}) - (\mathrm{V_H} + \frac{h_h}{2} \cdot \omega_H) \qquad \text{eq. (21)}$$

$$V_{rel,b1} = (V_{B2} - \frac{h_{b2}}{2} \cdot \omega_{B2}) - (\mathrm{V_{B1}} + \frac{\mathrm{h_{b1}}}{2} \cdot \omega_{B1}) \qquad eq. (22)$$

$$V_{rel,b2} = \left(V_{B3} - \frac{h_{b3}}{2} \cdot \omega_{B3}\right) - (\mathrm{V_{B2}} + \frac{h_{b2}}{2} \cdot \omega_{B2}) \qquad \text{eq. (23)}$$

$$V_{rel,b3} = V_s - (\mathrm{V_{B3}} + \frac{h_{B3}}{2} \cdot \omega_{B3}) \qquad eq. (24)$$

All parameters for this model came from the paper by Wu et al. (Wu, Jun, and Yi Qiu 2020) Now the bond graph for the passenger model is shown in Fig. 6.

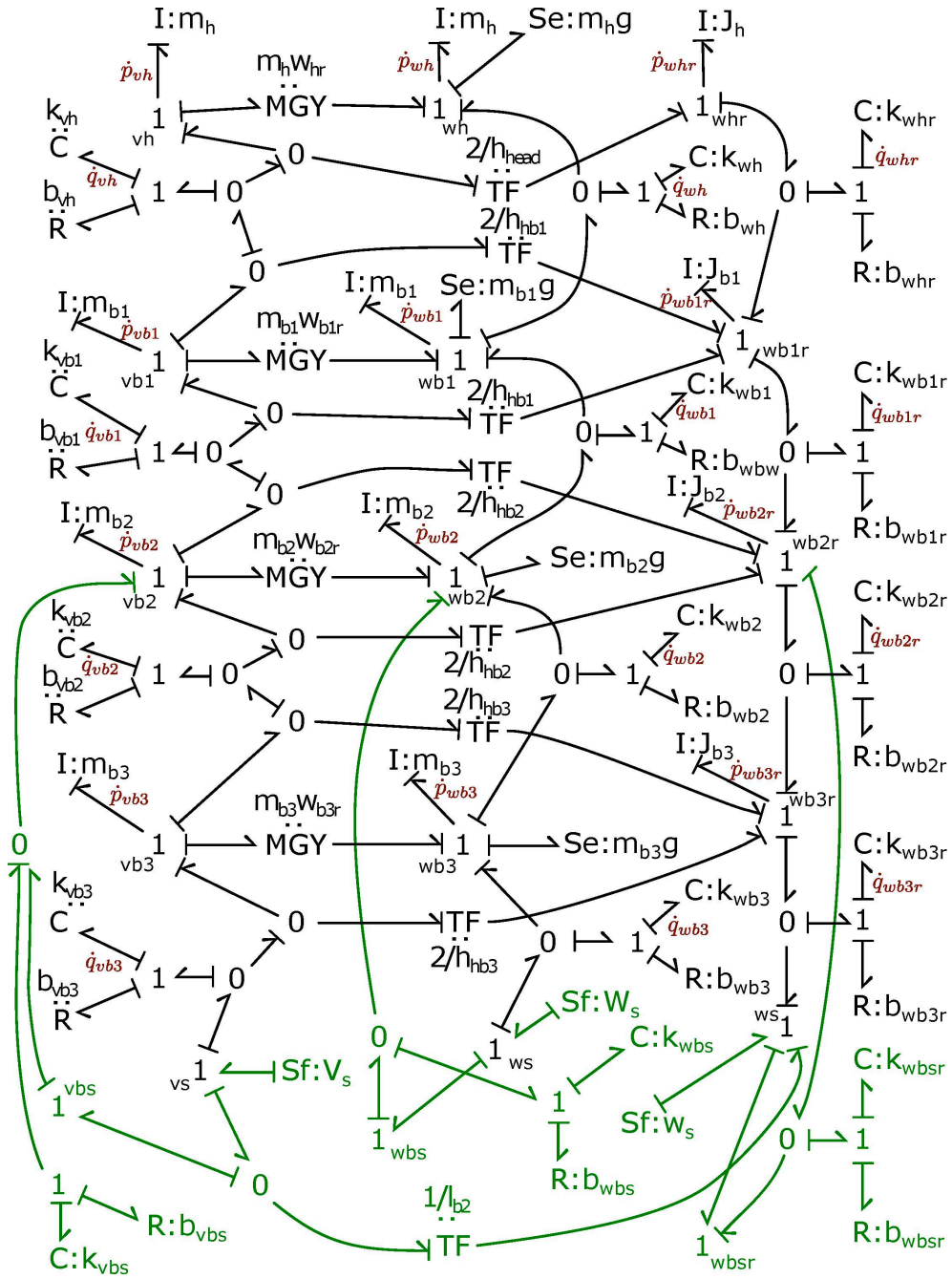

Figure 6: Bond graph of passenger model

2.3 Vehicle-Passenger combined model

The Vehicle-Passenger combined model was developed to obtain a passenger's head motion under a specified steering angle input.
At first, the relative position of the seat with respect to the vehicle's center of gravity is determined, as shown in Fig. 7.

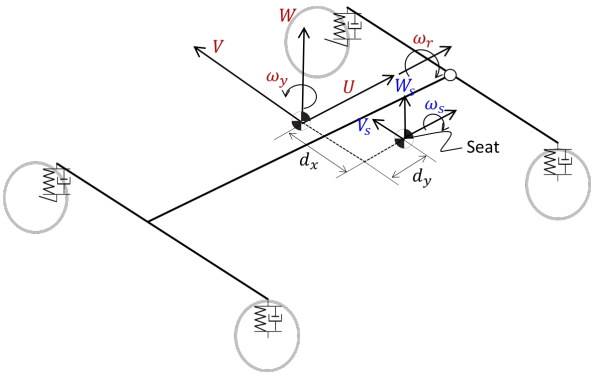

Figure 7: Relative seat position

The relative equations between the velocity of the vehicle and the velocity of the passenger's seat can be derived below.

$$V_s = V + d_y \cdot \omega_y \qquad \text{eq.(25)}$$

$$W_s = W - d_x \cdot \omega_r \qquad eq.(26)$$

Where:

V = lateral velocity of the vehicle

W = vertical velocity of the vehicle

V_s = lateral velocity of the seat

W_s = vertical velocity of the seat

ω_y = yaw rate of the vehicle

ω_r = roll rate of the vehicle

d_x = longitudinal distance from C. G of the vehicle to C. G of the seat

d_y = lateral distance from C. G of the vehicle to C. G of the seat

Having both the vehicle and the passenger model, the combined vehicle-passenger bond graph which is shown in Fig. 8, can be developed.

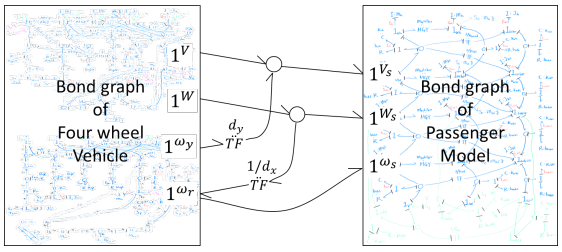

Figure 8: Vehicle and passenger connected bond graph

2.4 Validation for use of active bond in combined graph

To simplify the system, it is hypothesized that the reaction from the passenger onto the vehicle can be neglected since the passenger's momentum is significantly smaller than that of the vehicle's. This is incorporated through use of active bonds from the vehicle to the passenger model, this assumption is then verified for reasonability.

The simulation results are compared with active bond and normal bond, shown in Fig. 9. In the result plots, no significant difference is found between the two cases. This justifies the use of active bonds and allows for simplification of the equations of motion and subsequently reducing the simulation running time as much as 93% (44sec. → 3sec.)

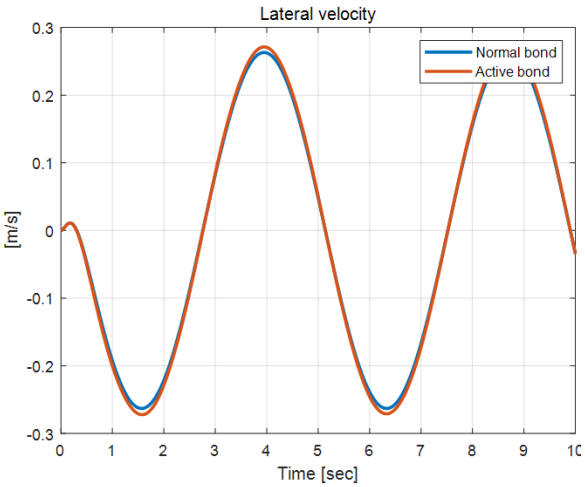

(a)

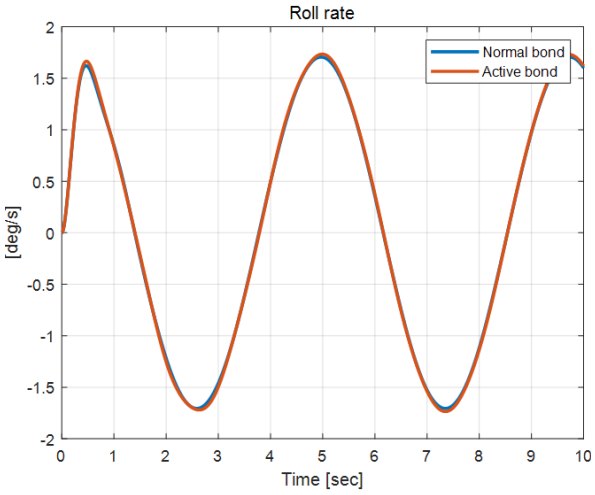

(b)

Figure 9: Comparison plot for vehicle's (a) lateral velocity, (b) roll rate

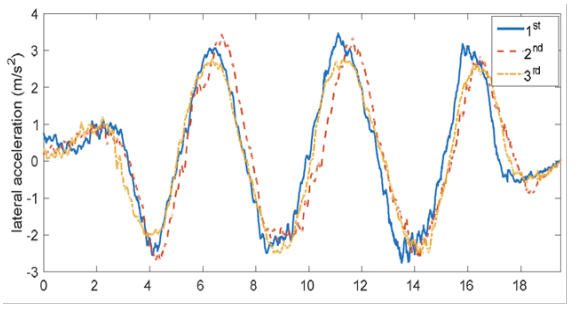

(a)

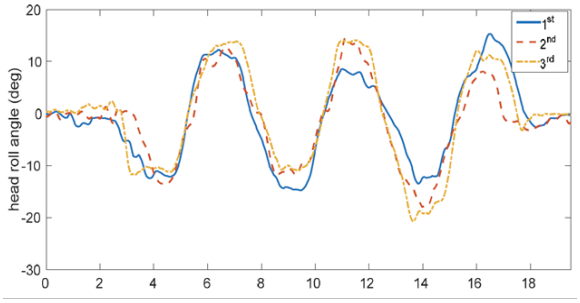

(b)

Figure 10: Experimental results for (a) Lateral acceleration, (b) Head roll angle (Zamzuri et al. 2018)

3 VALIDATION FOR VEHICLE-PASSENGER COMBINED MODEL

ZAMZURI, Hairi, et al. (Zamzuri et al. 2018) performed an experiment with a real car and passengers to estimate the transfer function between the passenger's head roll angle and the vehicle's lateral acceleration. In their experiment, a sinusoidal lateral acceleration input with an amplitude of 3m/s^2 and a frequency of 0.21Hz with a constant 30KPH vehicle speed has resulted in a passenger's head roll angle within a range of around ±15°. It is investigated whether the current simulation would replicate this experimental result. First, the steering angle profile that induced the same lateral acceleration profile as Hairi et al.'s experiment was found. Then the simulation result for the passenger's head roll angle was compared to that of the experiment's and it was concluded that the passenger model can sufficiently approximate the real passenger's head roll angle. Fig. 10. and Fig. 11 show the lateral acceleration and head roll angle profiles for Hairi's experiment and current simulation, respectively and it is noted that they display a somewhat similar behavior in terms of amplitude and frequency.

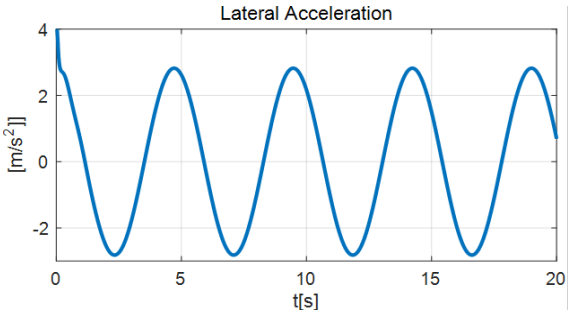

(a)

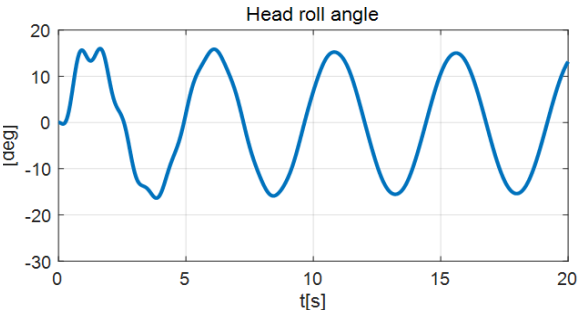

(b)

Figure 11: Simulation results for (a) Lateral acceleration, (b) Head roll angle

4 APPLICATION OF THE SVC MODEL

BLES, Willem (Bles, Willem 1998) said that motion sickness will be triggered when a discrepancy is detected between the subjective vertical which one estimates from previous experience, and the sensed vertical as determined from incoming sensory information. J.E. Bos and W. Bles (Bos, J.E., and W. Bles. 1998) use the term MSI (Motion Sickness Incidence) indicating the percentage of people who vomit after 2 hours of enduring motion versus frequency and acceleration of the head motion.

KAMIJI, Norimasa, et al. (Kamiji et al. 2007) made the 3D SVC (Subjective Vertical Conflict) model which can calculate the MSI (shown in Fig. 13). WADA, Takahiro, et al. (Wada and Kamiji 2015) expanded this model to 6DOF motion, including head rotation, by introducing the otolith-canal interaction.

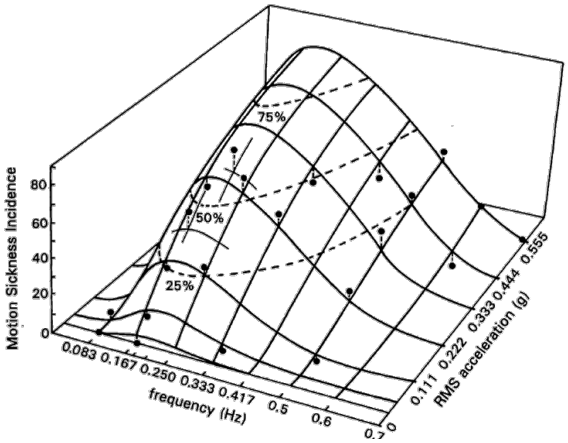

Figure 12: Motion sickness incidence (%) after two hours of endured motion versus frequency and acceleration. Each dot represents an observed average among 20 subjects (O'Hanlon, James F., and Michael E. McCauley 1973)

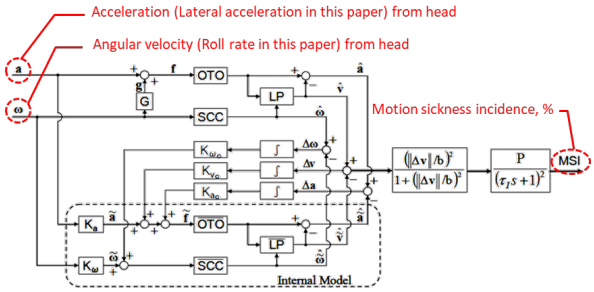

Figure 13: 3D SVC(three-dimensional subjective vertical conflict) model (Kamiji et al. 2007)

This model consists the OTO block which is the otolith organ, the SCC block which represents the semicircular canals and the LP block which is a low-pass filter. and there's the Internal Model which calculates the estimated sensory information from the head's movement. As a result, the discrepancy between the sensory information from the vestibular system and the estimated sensory information from the internal model generates motion sickness.

We can calculate the severity of motion sickness for a passenger sitting in a vehicle using this model by simply providing it with the roll rate and the lateral acceleration of the head. The final combined Simulink model is shown in Fig.14.

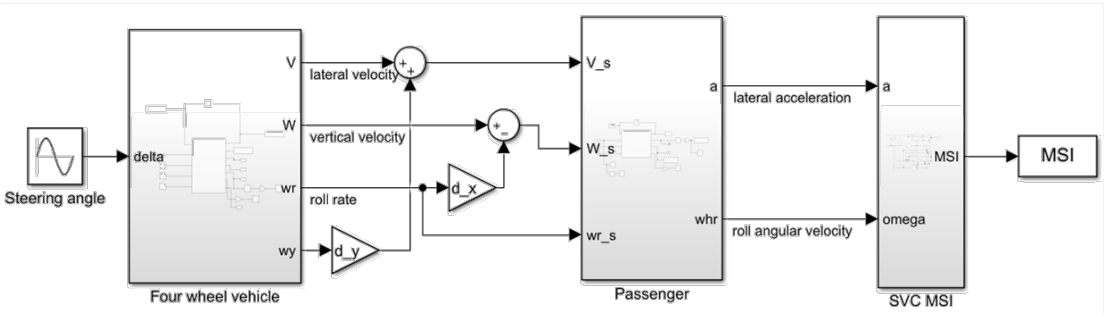

Figure 14: Combined Simulink model

5 UTILIZATION OF INTEGRATED MOTION SICKNESS MODEL

With this combined motion sickness model, we can estimate the severity of motion sickness under a variety of vehicle conditions. As brought in Table 1, various vehicle conditions with different sinusoidal steering inputs and vehicle speeds are investigated and their resulting MSI are then compared.

CASE	Vehicle speed	Steering angle	Steering frequency
CASE1-1	50kph	2deg.	0.3Hz
CASE1-2	50kph	4deg.	0.3Hz
CASE1-3	50kph	6deg.	0.3Hz
CASE1-4	50kph	8deg.	0.3Hz

(a)

CASE	Vehicle speed	Steering angle	Steering frequency
CASE2-1	40kph	5deg.	0.3Hz
CASE2-2	50kph	5deg.	0.3Hz
CASE2-3	60kph	5deg.	0.3Hz

(b)

Table 1: Test conditions for (a) Various steering angles, (b) Various vehicle speeds

The MSI results from the above various conditions are shown in Fig. 15. As shown in the plot, it is found that the passenger riding the car which has higher steering amplitude and vehicle speed experiences higher (worse) motion sickness.

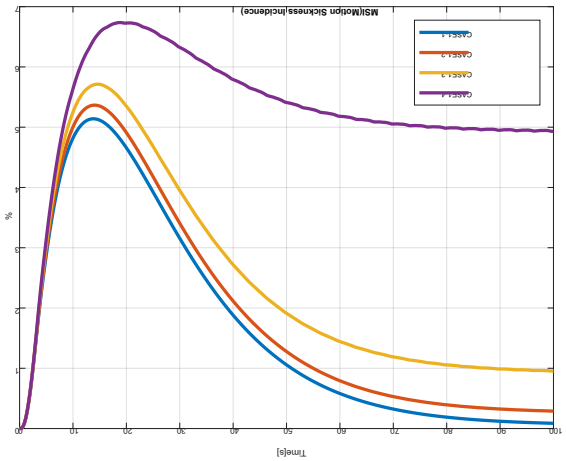

(a)

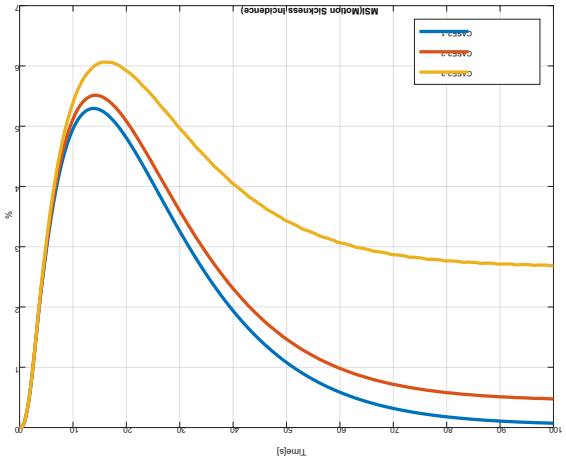

(b)

Figure 15: Motion sickness incidence under (a) Various steering angles condition, (b) Various vehicle speeds condition

6 CONCLUSION

A bond graph of a four-wheel vehicle model with an on-board passenger model were constructed for calculating the MSI, I.E., Motion Sickness Incidence. All bond graphs were causal and the concept of active bonds is employed to connect the vehicle bond graph to the passenger bond graph. This simplifies the system while preserving accuracy. The integrated vehicle-passenger model was later validated against experimental data. By using this combined model, the head motion of the passenger can be obtained for a specified steering angle, which is itself used to estimate the severity of motion sickness.

Access to a quantitative index for motion sickness allows for designing optimal controllers which could mitigate motion sickness in the future.

7 REFERENCES

Bles, Willem. 1998. "Coriolis effects and motion sickness modelling." *Brain research bulletin,* 47(5),pp. 543-549.

Bos, J. E., and W. Bles. 1998. "Modelling motion sickness and subjective vertical mismatch detailed for vertical motions." *Brain research bulletin,* 47(5), pp. 537-542.

Dugoff et al. 1970. "An analysis of tire traction properties and their influence on vehicle dynamic performance." *SAE transactions, 1219-1243.*

Kamiji et al. 2007. "Modeling and validation of carsickness mechanism." SICE Annual Conference. IEEE, 2007.

O'Hanlon, James F., and Michael E. McCauley. 1973. "Motion sickness incidence as a function of the frequency and acceleration of vertical sinusoidal motion." *CANYON RESEARCH GROUP INC GOLETA CA HUMAN FACTORS RESEARCH DIV.*

Wada, Takahiro, and Norimasa Kamij. 2015. "A mathematical model of motion sickness in 6DOF motion and its application to vehicle passengers." *arXiv preprint arXiv:1504.05261*

Wada, Takahiro et al. 2012. "Can passengers' active head tilt decrease the severity of carsickness? Effect of head tilt on severity of motion sickness in a lateral acceleration environment." *Human factors,* 54(2), 226-234.

Wu, Jun, and Yi Qiu. 2020. "Modelling of seated human body exposed to combined vertical, lateral and roll vibrations.". *Journal of Sound and Vibration*, 485, 115509.

Zamzuri, Hairi, Nurhafizzah Hassan, and Mohd Hatta Mohammed Ariff. 2018 "Modeling of head movements towards lateral acceleration direction via system identification for motion sickness study." In 2018 International Conference on Information and Communications Technology (ICOIACT), pp. 633-638. IEEE.

AUTHOR BIOGRAPHIES

EUNIL KIM is a Research Engineer of Hyundai Motor Company. He has been developing suspension system of the vehicle. He has studied about reduction of motion sickness by using suspension control in UC Davis. He is interested in vehicle dynamics and control. His email address is eunilk@hyundai.com.

ALI AKBARI is a PhD student of Mechanical Engineering at UC Davis where he researches ride comfort for vehicle occupants at Hyundai Center of Excellence. He received his BSc and MSc from Sharif University of Technology with a focus in biomechanics. His email address is alakbari@ucdavis.edu .

DONALD L. MARGOLIS is a professor of mechanical engineering and director of the Hyundai Center of Excellence in Vehicle Dynamics Systems & Control at UC Davis. He has extensive experience in teaching system dynamics at the graduate and undergraduate levels, consultation in vibration controls, and has published numerous papers on the industrial applications of dynamics. His email is dlmargolis@ucdavis.edu.